EXPERIMENTAL STUDY OF ROTATING STALL IN HIGH-PRESSURE STAGES OF AN AXIAL-FLOW COMPRESSOR

V. S. Beknev, A. V. Zemlyanskiy and
R. Z. Tumashev

Translation of: "Eksperimental'noye Issledovaniye Vrashchayushchegosya Sryva v Vysokonapornykh Stupenyakh Osevogo Kompressora," Mashinostroyeniye, No. 8, 1970, pp. 116-122.

NATIONAL AERONAUTICS AND SPACE ADMINISTRATION
WASHINGTON, D. C. 20546 SEPTEMBER 1973

STANDARD TITLE PAGE

1. Report No. NASA TT F-15,115	2. Government Accession No.	3. Recipient's Catalog No.
4. Title and Subtitle EXPERIMENTAL STUDY OF ROTATING STALL IN HIGH--PRESSURE STAGES OF AN AXIAL-FLOW COMPRESSOR		5. Report Date SEPTEMBER 1973 6. Performing Organization Code
7. Author(s) V. S. Beknev, A. V. Zemlyanskiy and R. Z. Tumashev		8. Performing Organization Report No. 10. Work Unit No.
9. Performing Organization Name and Address Techtran Corporation P.O. Box 729 Glen Burnie, Maryland 21061		11. Contract or Grant No. NASw-2485 13. Type of Report and Period Covered Translation
12. Sponsoring Agency Name and Address National Aeronautics and Space Administration Washington, D. C. 20546		14. Sponsoring Agency Code

15. Supplementary Notes

Translation of: "Eksperimental'noye Issledovaniye Vrashchayushchegosya Sryva v Vysokonapornykh Stupenyakh Osevogo Kompressora," Mashinostroyeniye, No. 8, 1970, pp. 116-122.

16. Abstract

Results of an experimental study of rotating stall in axial-flow compressor stages with different types of profiling along the blade height and with different calculated regimes of flow past a profile in the cascade. It is found that, in spite of the different safety margins with respect to boundary layer separation in the cascades of the different stages, their boundaries of stable operation are almost the same. It is shown that profiling taking into account end effects has a stabilizing influence and leads to a smoother transition to the rotating stall regime. The flow in rotating stall zones is shown to be of three--dimensional nature. It is shown that this three-dimensional structure can be detected with the aid of straight and L-shaped tensoanemometer probes.

17. Key Words (Selected by Author(s))	18. Distribution Statement
	Unclassified-Unlimited

19. Security Classif. (of this report)	20. Security Classif. (of this page)	21. No. of Pages	22. Price
Unclassified	Unclassified	9	

EXPERIMENTAL STUDY OF ROTATING STALL IN HIGH-PRESSURE STAGES OF AN AXIAL-FLOW COMPRESSOR

V. S. Beknev, A. V. Aemlyanskiy and
R. Z. Tumashev

Investigation of rotating stall in axial compressors is aimed at solving /116* the problem of dynamic strength, expanding the range of stable operation, and also at obtaining additional information about the character of flow. Investigations [1, 2] have established the influence of various geometrical dimensions of stages on the parameters of rotating stall. Except for [3], however, in which 2 versions of an axial compressor, profiled according to the laws of constant circulation ($c_u r$ = const) and "solid" ($\frac{c_u}{r}$ = const), the literature contains no data on the influence of the law of profiling of the blades with respect to radius on the left-hand characteristic of the stage, position of the boundary of stable operations and conditions of the development of zones of rotating stall.

Presented in this article are some results of an experimental investigation of rotating stall in four stages of an axial compressor, designed for $\bar{d}_i = 0.7$; $D_k = 0.33$ m and aspect ratio $\bar{h}_{rc} \simeq 1.4$ on the following parameters at the design point: $\bar{H}_t = 0.5$; $C_a = 0.5$ and $\tau' = 0.5$. Arrays were selected for 2 of the 4 investigated stages for the nominal mode of flow past the profile, and mode of maximum profile quality K_{max} for the other two. /118 In the nominal flow mode and in the mode K_{max} the blades were profiled with respect to radius both by the law $c_u r$ = const, and in consideration of end effects. The flow part of the experimental compressor was assembled by the rotating guide vane + rotor + + guide vane + straightening vane and each version had different rotor + guide vane links, the geometric parameters of which are presented in Table 1.

*Numbers in the margin indicate pagination in the foreign text.

TABLE 1. GEOMETRIC PARAMETERS OF EXPERIMENTAL COMPRESSOR STAGES.

Legend: No. of version	Profiling method	$\bar{r}$	Rotor					Guide				
			$\theta°$	$\vartheta°$	b/t	b, мм	Z	$\theta°$	$\vartheta°$	b/t	b, мм	Z
1	$c_u r \neq$ const, K_{max}	0,72	87	68	1,6	39,8	30	78	51	1,54	37,3	31
		0,85	60	60	1,21	35,5		63	58	1,29	36,8	
		0,98	48	42,5	1,02	34,6		64,5	59	1,29	42,5	
2	$c_u r =$ const, K_{max}	0,72	79,5	70,5	1,35	33,2	30	67,4	53,3	1,44	35,0	31
		0,85	59,3	59,0	1,30	38,1		61,7	57,5	1,33	38,0	
		0,98	49,5	47,0	0,97	33,0		59,5	61,4	1,23	40,5	
3	$c_u r =$ const, nominal	0,72	69,0	79,9	2,16	32,5	50	48,7	56,7	2,6	38,1	51
		0,85	44,3	61,0	2,17	38,3		47,6	59,7	2,37	41,0	
		0,98	27,4	45,9	1,66	33,9		48,3	61,5	2,01	40,1	
4	$c_u r \neq$ const, nominal	0,72	69,0	78,5	2,65	40	50	48,5	55,3	2,73	40	51
		0,85	48	61,3	1,92	34		51,5	59,0	2,11	36,6	
		0,98	35,6	42	1,79	36,5		48,0	62	2,22	44,4	

Commas indicate decimal points.

For the purpose of reducing the overall diffusion of the flow the tube was made conical from the rotor to the straightening vane to achieve $C_{3a} \simeq C_{1a}$. The intake guide vane, with number of blades z = 16 and thickness b/t = 0.3, deflected the flow in rotation by ≈14°, and the straightening vane, with z = 8 and b/t = 1.15, ensured axial discharge of the flow. The relative axial space $\bar{S}_z = S_z/b_{rc}$ for all of the investigated variants were $\bar{S}_{z_1} = S_{z_2} \approx 1.0$. The measuring cross-sections were placed at 1/2 the axial space.

In order to determine the characteristics of the investigated variants in the form of the functions $\bar{H}_{ad} = f(\bar{C}_a)$ and $\eta^*_{ad} = f(\bar{C}_a)$ we use a 5-band

full-pressure probe with an adjustable center band, installed in the cross-section behind the rotor.

A peculiarity in the operation of the experimental compressor — intake and exhaust of error in the room and rather high peripheral velocity $u_{k_{pr}} = 180$ m/sec ($n_{rk} = 175$ revolutions per second) required that the primary instrument be a low-inertial apparatus whose sensing element has a high frequency of free oscillations and stable characteristics under conditions of air pollution. Two types of probes were manufactured as the primary instrument: a full-pressure membrane probe, similar to one described in [4], and a tensoanemometer, developed and first used by V. S. Knyazev. Further investigations were conducted with tensoanemometers, since the membrane strain gauge pressure probes lost their sensitivity during tests due to pollutants. The sensing element of the tensoanemometer was a plate, attached on one end, and strain gauges, protected from the action of the flow by a cover, which was an extension of the clamp, were cemented to the plate at the clamping point. Part of the length of the plate, not covered by the strain gauges, extended into the flow and was bent under the influence of the dynamic pressure of the flow, equal to $\frac{\rho V^2}{2}$, which changed the resistance of the cemented strain gauge and the output signal level of the amplifier of the strain gauge system. The free frequency of the plate, one end of which was clamped, was

$$f = \frac{1{,}014\,\delta}{l^2}\sqrt{\frac{Eg}{\gamma}}\ \text{Hz},$$

where δ is the thickness of the plate, l is its length, E is the modulus of elasticity, γ is density and g is the acceleration of gravity.

The free frequency of the plate, made of getinax with $l = 12$ mm, $\delta = 1$ mm, was $\simeq 5000$ Hz.

In addition to the tensoanemometers, recording pulsations of axial and peripheral velocity components, V-shaped probes were also made, the plate of which was perpendicular to the axis of the clamps and recorded pulsations of only the radio component of velocity. The tensoanemometers were subjected to static calibration in the tube and dynamic calibration in the pulsating flow.

Thus the low-inertial apparatus made it possible to determine the parameters of rotating stall (the number of zones i_z and their velocity $\bar{\omega}_z$) and three--dimensional pattern of flow in a zone. A diagram of the compressor and apparatus is shown in Figure 1.

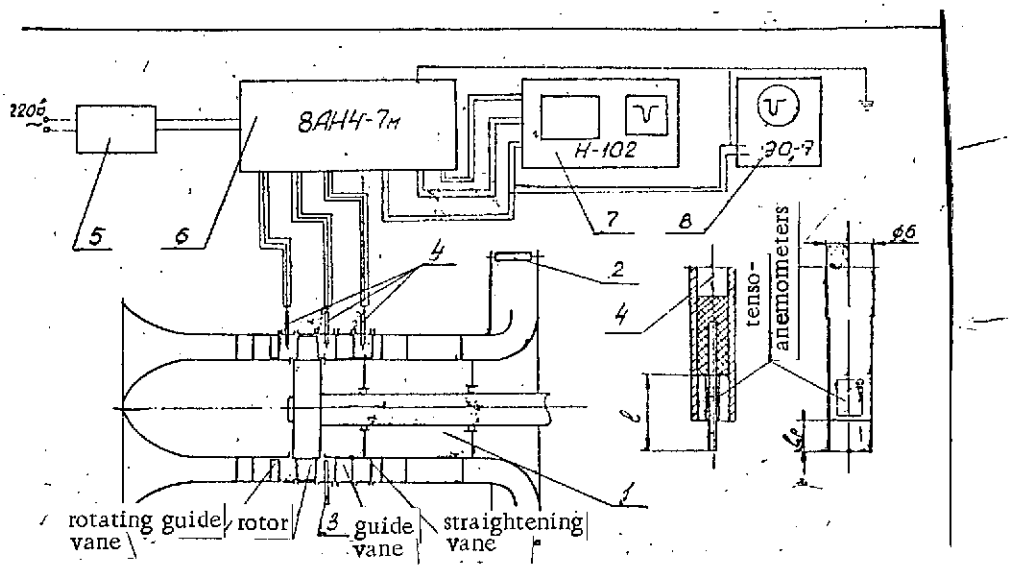

Figure 1. The Diagram of Experimental Compressor and Measuring Apparatus: 1, compressor; 2, throttle system; 3, 5-band full-pressure probe; 4, tenso-anemometer; 5, power unit; 6, amplifier; 7, loop oscillograph; 8, electronic oscillograph. /119

The characteristics of the rotors of the two stages of the first and third variants are presented in Figure 2, and the parameters of rotating stall modes are given in Table 2, where $\bar{C}_{ab}$ and $\bar{H}^*_{adb}$ are the flow rate and adiabatic head coefficients at the boundary of stable operations, and f_d is the frequency of the process, recorded by the tensoanemometer. The boundary of stable operation for the investigated compressor stages varied within the range of $\bar{C}_{ab}$ = 0.435 to 0.45, and the stages with the arrays assembled for the nominal mode of flow past the profile changed over to the rotating stall mode with several smaller flow rates. /120

Three forms of rotating stall were observed in all the investigated stages, but with a different degree of stability: weak multizonal stall with a high relative rate of rotation and two forms of unizonal stall with different velocity of propagation.

Transition to the left part for stage 1 (Figure 1) was accompanied by the appearance of weak two-zone stall with $\bar{\omega}_z = 0.693$, which changed to four-zone stall as the flow rate decreased, and then for $\bar{C}_a = 0.36\text{-}0.30$ unizonal stall with $\omega_z = 0.354\text{-}0.293$ appeared, which at $C = 0.3$ changed to a different unizonal stall $\bar{\omega}_z = 0.235$ with strong ejection and sharp drop of $\bar{H}^*_{ad}$. Unizonal stall $\bar{\omega}_z = 0.232$, with a substantial drop of $\bar{H}^*_{ad}$ and strong ejection of the flow into the space in front of the rotor, was immediately observed for the third stage.

During investigation of the third stage it was possible only by extremely slow throttling to obtain a model of multizonal stall, which changed to a unizonal stall with $\bar{\omega}_z = 0.37$ in a very narrow range of flow rate (point A in Figure 1 and Table 2), afterwhich stall with $\bar{\omega}_z = 0.232$ appeared. In reverse these forms of rotating stall do not appear. In stage 1 in reverse the pattern was repeated in the reverse sequence, i.e., all 3 forms of rotating stall appeared.

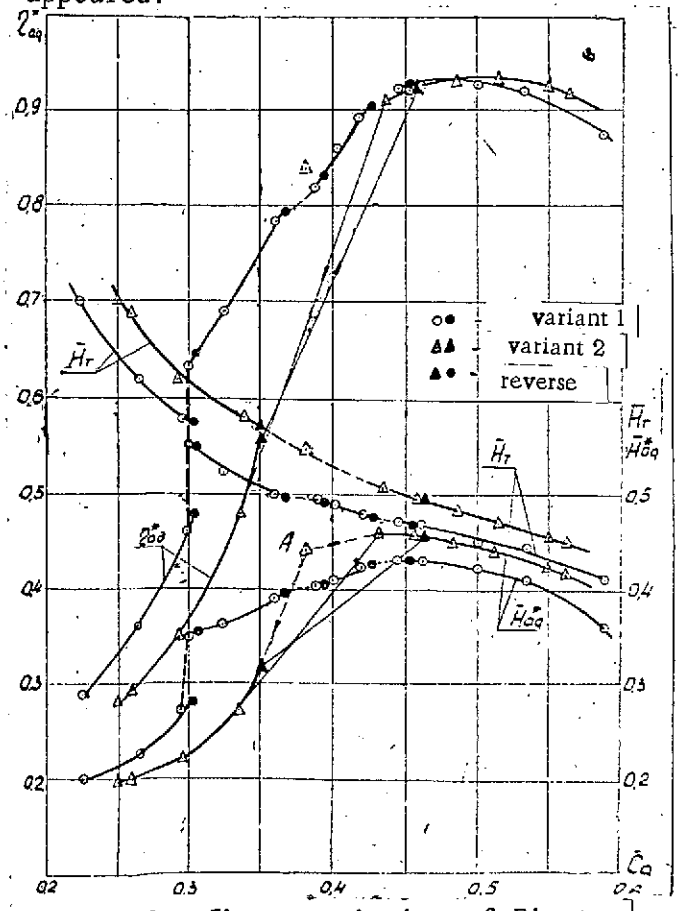

Figure 2. Characteristics of First and Second Stage Rotors.

Thus, transition of the third stage rotor to the left side in comparison with the first stage rotor, is accompanied by a steeper characteristic, distinct hysteresis phenomena and considerable discontinuity with respect to flow rate. For the fourth stage, different from the third stage in that its peripheral tube has greater thickness, the transition was accompanied by the appearance of 3 zone flow with $\bar{\omega}_z = 0.705$, and as the flow rate decreases the number of zones increase to 4, and then to 5 and even a sixth zone model was observed before the appearance of

single-zone stall with $\bar{\omega}_z = 0.365$; for $\bar{C}_a = 0.325$ a single-zone stall appeared with $\bar{\omega}_z = 0.212$ and strong ejection.

The form of the characteristic of the second stage rotor is similar to that of the first stage but is steeper in the multizone stall mode with unstable transition from the multizone flow mode to the single-zone and conversely. An oscillogram of such oscillation is shown in Figure 3b, where transition from single-zone stall (the time axis extends from right to left) to multizone stall is recorded and one zone breaks up into 5 zones, which gradually occupy a symmetrical position on the circumference. The stages that were profiled with consideration of end phenomena had a smoother transition to the left side with a more stable left side characteristic.

TABLE 2. PARAMETERS OF ROTATING STALL MODES OF COMPRESSOR STAGES. /121

No. of variants	c_a b	h_{ad} b	Multizone					First kind single-zone				Second kind single-zone			
			$\bar{c}_a$	$\bar{h}^*_{ad}$	i_z	$\bar{\omega}_z$	f_d,Hz	$\bar{c}_a$	$\bar{h}^*_{ad}$	$\bar{\omega}_z$	f_d,Hz	$\bar{c}_a$	$\bar{h}^*_{ad}$	$\bar{\omega}_z$	f_d,Hz
1	0,445	0,435	0,42	0,425	2	0,693	241	0,361	0,393	0,354	61,6	0,295	0,281	0,235	40,9
			0,41	0,405	3	0,690	360	0,325	0,360	0,319	55,5	0,265	0,225	0,203	35,4
			0,385	0,400	4	0,687	479	0,300	0,350	0,293	51,0	0,225	0,200	0,195	33,9
2	0,450	0,429	0,430	0,412	2	0,685	237	0,377	0,413	0,395	68,8	0,290	0,258	0,249	42,3
			0,400	0,399	3	0,681	356	0,350	0,395	0,370	64,4	0,242	0,224	0,209	36,4
			0,380	0,372	4	0,680	474	0,305	0,373	0,320	56,8	0,175	0,182	0,189	32,8
3	0,440	0,460	0,374	0,430	4	0,715	498	0,380	0,430	0,370	64,3	0,337	0,280	0,232	40,2
					5	0,716	623					0,295	0,220	0,197	34,2
					6	0,714	746					0,25	0,200	0,186	32,3
4	0,435	0,443	0,388	0,405	3	0,705	361	0,370	0,390	0,365	63,5	0,325	0,232	0,212	36,8
			0,380	0,385	4	0,705	492	0,355	0,381	0,350	61,0	0,290	0,193	0,195	33,9
			0,370	0,371	5	0,703	614	0,325	0,403	0,331	57,7	0,28	0,184	0,185	32,2

Commas indicate decimal points.

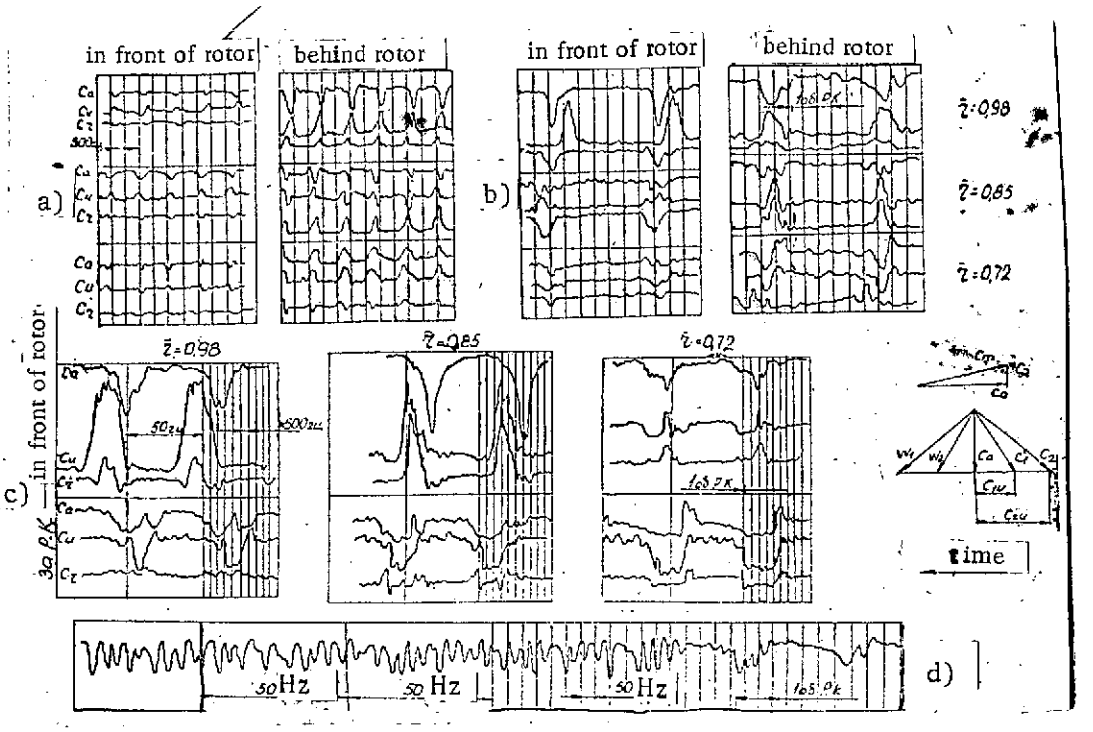

Figure 3. Oscillograms of Rotating Stall: a, Multizone Stall $i_z = 2$, $\omega_z = 0.685$, $\bar{C}_a = 0.425$; b, Single-zone Stall $\omega_z = 0.38$, $\bar{C} = 0.37$; c, Single-zone Stall $\omega_z = 0.235$, $\bar{C}_a = 0.27$; d, Transition from Single-zone Stall with $\omega_z = 0.39$ to Multizone $\bar{C}_a = 0.380$

Oscillograms of the pulsations of the axial, peripheral and radio components of velocity are shown in Figure 3a,b,c for 3 forms of rotating stall in the cross-sections in front of an behind the rotor on 3 radii for the second stage. The pulsations that extend upward on the oscillogram coincide with the velocity components (velocity triangles, Figure 3). The oscillograms show that very weak perturbations spread upward through the flow from multizone stall, and this is confirmed by the 5-band pneumatic probe installed in front of the rotor /122 (the total pressure diagrams at the rotor intake for the stable mode and multizone stall mode are practically the same), and that the amplitudes of the pulsations of the 3 velocity components are commensurable values.

Conclusions

1. In spite of the different margin for boundary layer separation in arrays of stages (different modes of flow past the profile), their stable operation boundaries are similar in magnitude.

2. Profiling with consideration of end effects has a stabilizing influence on the left-hand rotor characteristic and facilitates smoother transition to the rotating stall mode.

3. Flow in rotating stall zone, both in front of and behind the R.K., is three-dimensional in nature.

4. The use of straight and V-shaped tensoanemometer probes makes it possible to explain the spatial structure of flow in rotating stall zones.

REFERENCES

1. Borisov, G. A., Ye. A. Lokshtanov and L. Ye. Ol'shteyn, "Rotating Stall in Axial Compressor," *Promyshlennaya Aerodinamika*, No. 24, Oborongiz, 1962.
2. Yershov, V. N., *Neustoychivyye Rezhimy Turbomashin* [Unstable Modes of Turbines], "Mashinostroyeniye" Press, Moscow, 1966.
3. Luza, T. N. and W. D. Rannie, "Experimental Investigations of Propagating Stall in Axial Flow Compressor," *Trans. ASME*, Vo.. 76, No. 3, 1954.
4. Gorodetskiy, O. A., "Probe for Investigating Transient Processes in Centrifugal Compressors," in the book: *Kompressorniye i Kholodil'noye Mashinostroyeniye* [Compressor and Refrigeration Machine Building], No. 2, "TsINTIkhimneftmash" Press, Moscow, 1967.

Translated for the National Aeronautics and Space Administration under Contract No. NASw-2485 by Techtran Corporation, P.O. Box 729, Glen Burnie, Maryland, 21061; translator; Orville E. Humphrey.